NANOSECOND PULSE DIELECTRIC BARRIER DISCHARGE PLASMA ACTUATION IN SUPERSONIC FLOW

by

Amanda Kathryn Davis

A Thesis Submitted to The Honors College

In Partial Fulfillment of the Bachelors degree
With Honors in

Engineering Physics

THE UNIVERSITY OF ARIZONA

MAY 2012

Approved by:

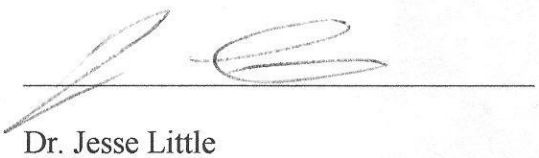

Dr. Jesse Little
Department of Aerospace & Mechanical Engineering

STATEMENT BY AUTHOR

This thesis has been submitted in partial fulfillment of requirements for a degree at The University of Arizona and is deposited in the University Library to be made available to borrowers under rules of the Library.

Signed: 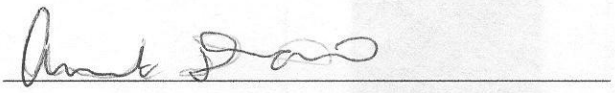

Abstract

Boundary layer control is a topic of constant concern in the area of aerodynamics. This study addresses a possible new method of affecting boundary layers and shock structure in supersonic flow. Nanosecond pulse dielectric barrier discharge plasma actuators are tested on a flat plate in a supersonic wind tunnel. Effects were observed using schlieren imaging to analyze changes in density gradients in the flow. While no noticeable results were found, the flow Mach numbers and electrical characteristics tested were very limited in variety due to complications with discharge formation and plate design. Much was learned to suggest improvements for further testing and this will facilitate later tests of similar technologies in this area of interest.

Acknowledgments

This study would not have been possible without the contributions of several other individuals. I would like to thank Dr. Jesse Little for his guidance and encouragement, and for sharing his expertise and ideas for this project. I am also very grateful to Rob Dawson for sharing his knowledge of schlieren imaging and the pulser setup, but especially for his advice and willingness to work long hours with me to help see it through to completion. Additionally, I would like to thank Kyle Sheets for his work on the flat plate design, Brian Franz for his support in running the supersonic wind tunnel, and Cheryl Blomberg for her help with the wind tunnel and pulser setup.

I. Introduction

Fluid flow over solid surfaces is a consistent, significant issue in many engineering applications. It comes into play in such areas as pipe flow, engine design, and the aerodynamics of automobiles and airplanes. While some basic principles hold true across the board, more specific characteristics of the flow and surfaces studied can vary a great deal depending on the purpose for which they are intended. For example, one distinct type of flow, supersonic flow, is primarily discussed in reference to rocket and jet engines or to the aerodynamics involved in the flight of aircraft and projectiles. It is this kind of flow that was predominantly researched and which will be discussed in this study.

However, before there is an in-depth discussion of supersonic flow, it is important to discuss a few of the broader issues of fluid flow. In general, as a fluid flows over a stationary, solid body, the fluid far from the body flows relatively unperturbed by the existence of the body. For experimental purposes (like in a wind tunnel), there is a fairly consistent, steady speed and direction of this fluid flow—these two characteristics describe its freestream velocity, U_∞. However, the fluid near the body is forced to flow around the body somehow, thus altering its speed and direction compared to the rest of the flow. Besides this, the fluid directly touching the body experiences a frictional force from the surface and is considered to be stationary with regard to the body. This translates to an infinitesimally thin layer of fluid moving with the same speed and direction as the body, which means that a stationary body yields a stationary layer. This idea is called the no-slip condition, meaning the flow at the surface has the velocity of the surface. There must logically be some transition region between this stationary layer and the fluid flow far from the body where the velocity is somewhere between the two. This transition layer is called the boundary layer.

Boundary layers are typically described as laminar or turbulent. The transitional state between the two will not be considered here. Laminar boundary layers have a smoother transition between the stationary flow directly next to an object and the rest of the flow. Friction drag depends on the change in the fluid velocity parallel to the object's surface in the direction perpendicular to the surface (*du/dy*). Laminar boundary layers create less drag than turbulent boundary layers. This makes them profitable in many situations. Turbulent boundary layers have the infinitesimally thin no-slip layer, followed by a region characterized by vortices and other complex structures that are difficult to understand or simulate precisely. These many disturbances give a large *du*/*dy*, which translates into greater drag. Thus, it would initially appear that laminar boundary layers would always be favorable.

However, there is another effect that must be taken into account before this conclusion can be reached. Variations in flow speed are always accompanied by variations in pressure, so pressure gradients are a constant feature of boundary layers. In certain geometries and flow speeds, this pressure variation can become such that, in part of the boundary layer, it starts pushing in the opposite direction of the rest of the flow. This is known as an adverse pressure gradient, and it leads to an effect called separation. Separation occurs when these gradients cause the flow to detach from the object, leaving a large pocket of air with much lower velocity between the object and the flow still traveling with U_∞. This separation drastically decreases any lift that might have been generated and increases drag on the object. Most studies in aerodynamics are particularly interested in avoiding separation, whether the object in question is an automobile, an airplane, or a golf ball. Turbulent boundary layers, because of the greater momentum of the air that comprises them, are less susceptible to these pressure gradients and therefore typically result in flow that stays attached over a longer distance than laminar boundary

layers, given the same shape and flow speed. Thus, turbulent boundary layers are often preferred if there is a risk of separation, as the increased drag initially induced by the turbulent layer is still much less than the drag caused by separation.

In supersonic flow, these same boundary layer characteristics apply. However, flow is additionally complicated by the presence of shocks. Information in air can only travel as fast as the speed of sound, so while subsonic fluid can adjust to flow smoothly around an object, supersonic flow cannot "see" the object coming until it reaches it. Then, with any change in geometry or flow there is a very sudden change in speed and pressure called a shock. The strong pressure gradient involved in the shock can induce separation, causing the same issues that occur with subsonic separation.

Much research has been done, and continues to be undertaken, that relates to boundary layer control. One example of this is intentionally transitioning from a laminar to a turbulent boundary layer in particular regions. Commonly discussed methods include "tripping" the air flow by adding small solid structures or unevenness to the surface of the object to increase frictional forces. Other methods attempt to provide additional momentum to allow the boundary layer to overcome regions of adverse pressure gradient. Examples include steady blowing/suction or periodic/pulsed momentum addition[5]. Another method, and the one primarily discussed here, is to use plasmas created by actuators placed directly on the surface of the object. In this case, the plasma can generate momentum or rapid localized heating depending on the excitation signal.

The actuators used here are Dielectric Barrier Discharge (DBD) actuators. They consist of two copper tape electrodes separated by a dielectric layer. The actuator geometry is asymmetrical, with a 0.5"-wide copper electrode placed directly on the object surface, the

dielectric layer on top of this, and a 0.25”-wide copper electrode placed on top of the dielectric, with its back edge even with the front edge of the half-inch electrode. The actuators can vary greatly in length, depending on the span of the object for which they are intended. A side-view of the actuator is shown in Figure 1.

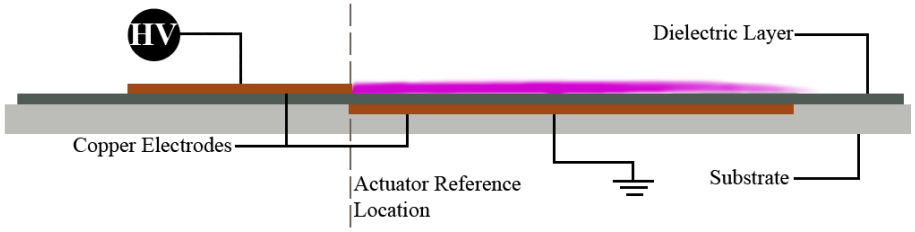

Fig. 1. High voltage pulses are applied to the “HV” electrode depicted above. The plasma is illustrated as the purple glow above, and it forms and heating occurs in the location shown (figure taken from Reference 1).

When in use, high voltages are applied to the top copper electrodes with the lower electrode grounded, so an electric field is generated. This field is strong enough to ionize the air near it, creating plasma (represented by the purple glow in Figure 1) in the region above the 0.5” electrode. The characteristics of the plasma are affected by the type of electrical signal applied to the system. The two primary types used are alternating current (AC) and nanosecond pulse (NS) signals.

Most research on these actuators has been performed with AC plasmas. The signal sent in to the system is a regular sine wave of a certain frequency and voltage, though these two electrical characteristics have been varied to observe their effects on the plasma and surrounding air flow. The electric field generated by this signal first ionizes the air to create the plasma, and then accelerates the ions to create an effect much like the blowing described by Greenblatt and Wygnanski[5]. This adds momentum to the boundary layer in lower velocity flows (U_∞ ~ 30 m/s)

and has been shown to facilitate reattachment of flow at different angles of attack when actuated with an appropriate frequency[2].

More recently, NS plasmas have been tested in similar situations. The electrical signals employed in these cases originate as square waves. These are passed to a "pulser" to signal the release of compressed high voltage pulses with durations of approximately 100 ns. A sample of the current and voltage associated with these pulses is shown in Figure 2(a). The plasmas generated by these signals, however, behave differently than the AC plasmas. While AC plasmas are accelerated themselves and thereby add momentum to the flow in a blowing fashion, the net velocity added by NS plasmas is negligible[3]. However, the NS plasmas still prove to be effective (sometimes even more so) in controlling flow over an airfoil and assisting in reattachment[3], so some other physical mechanism must be at work. One common theory about the underlying physics is that the generation of plasma causes extreme localized heating, which in turn causes compression waves that alter flow in the surrounding area. Examples of these waves can be seen in Figure 2(b). Based on the frequency with which the actuators are fired and inherent "characteristic frequencies" in the flow, the actuators can excite large vortices that entrain momentum into flow areas that would otherwise be still due to separation, thereby increasing lift and decreasing drag on airfoils at corresponding angles of attack[3]. These NS plasmas have proven to be effective at Re up to 1.15M[3] and Mach up to 0.85 [4]. The have also been used to modify shock structure over a cylinder at Mach 5[6].

The purpose of this study was to examine the effects of NS DBD plasma actuators at even higher velocities (and lower pressure), in the supersonic range. As described earlier, this region is characterized by distinctive shocks that occur wherever there are quick changes in flow direction. In these tests, actuators are employed on the surface of a flat plate to observe their

effects on the boundary layer and shock structure. This work is intended to lay a foundation for future work on the control of shock boundary layer interaction (SBLI).

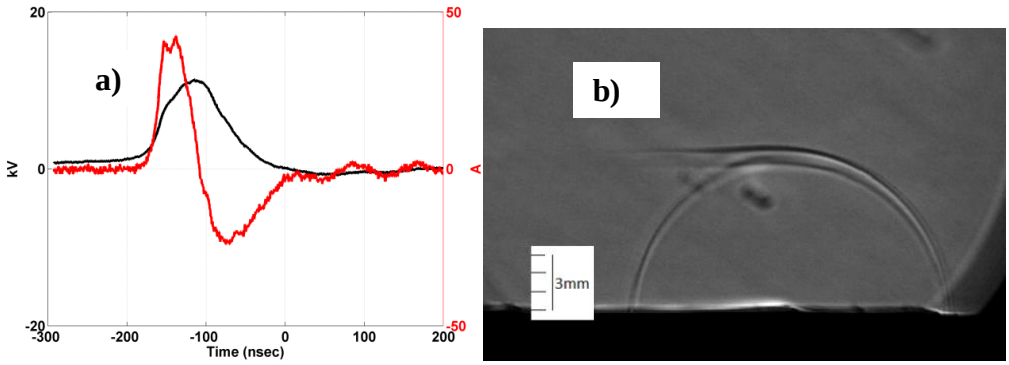

Fig. 2. (a) Sample voltage and current waveforms applied to the actuator and (b) compression waves formed as a result. Both images are for nanosecond pulses applied to a 20 cm DBD load at 1 kHz (taken from Ref. 1).

II. Experimental Facilities and Techniques

The supersonic flow experiments described here were conducted in The University of Arizona Department of Aerospace and Mechanical Engineering supersonic wind tunnel. The tunnel is capable of flow speeds between Mach 1.5-5. It is a suction tunnel with flow generated by a vacuum chamber at the back end. Mach number is adjusted through the use of a converging diverging nozzle with variable throat and diffuser. The constant area test chamber on the tunnel is 3" wide, 4.75" tall, and 18" long.

The tests were run on a specially-designed flat plate, shown in Figure 3. The apparatus had a flat, 8"-long top surface that began with a sharp point at the front tip and sloped down at a 16º angle to a final thickness of 0.38". From there, the bottom portion was also flat, except for a half-cylindrical tube in the center. The tube started with a solid front as a continuation of the 16º slant, and then progressed to the end of the tube as a full half-cylinder. (The geometry for these

sections was chosen to optimize shock formation and location on the underside of the plate.) Behind the back edge of the flat plate, the half-cylinder turned into a full cylinder and extended for another 3.5” before going through a 90º turn. The end of this cylinder attached to a thin cylinder that fit in place in the wall plug of the wind tunnel. The attachment method was a hand tightened nut and pin arrangement to prevent relative rotation between each component in the assembly. The model was held stationary with respect to the tunnel by friction pins. Pictures of the components and the setup used are shown in Figure 3.

(a)

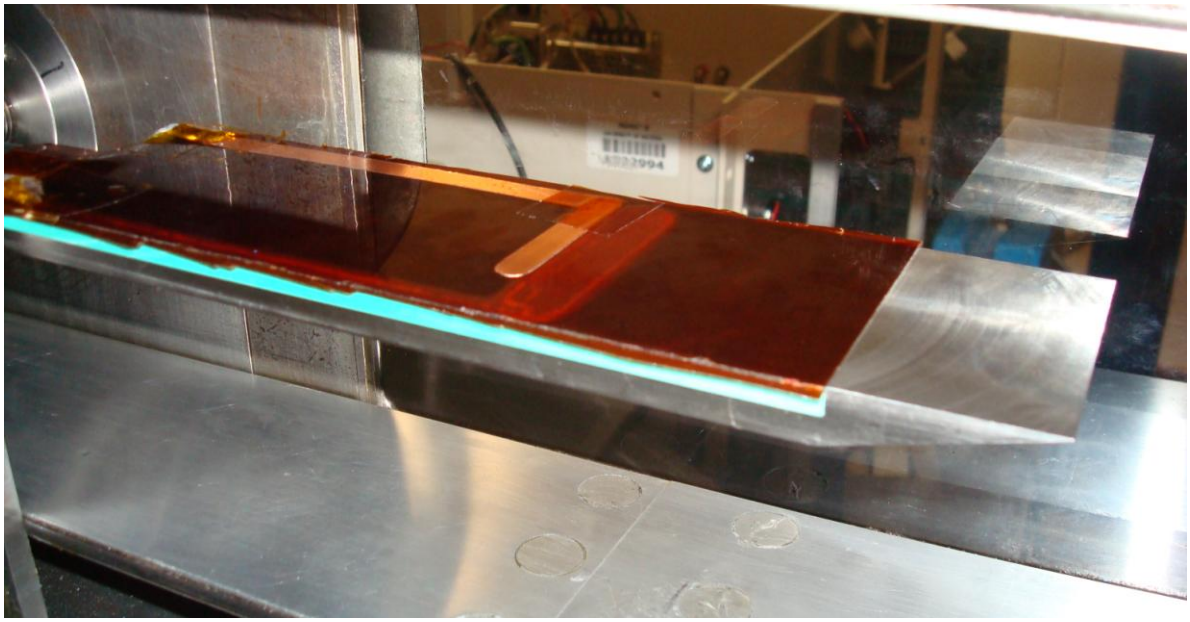

Fig. 3. (a) Flat plate used for plasma experiments, shown in wind tunnel. (b) Electrical connections and hand-tightened nut. (c) Hand-tightened nut shown with external seal in plug in the sidewall of the wind tunnel.

(b)

(c)

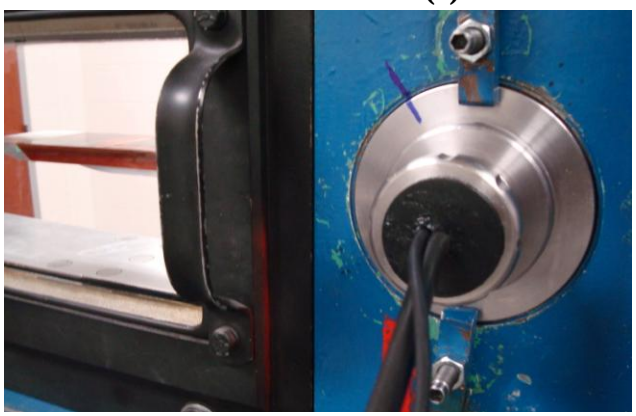

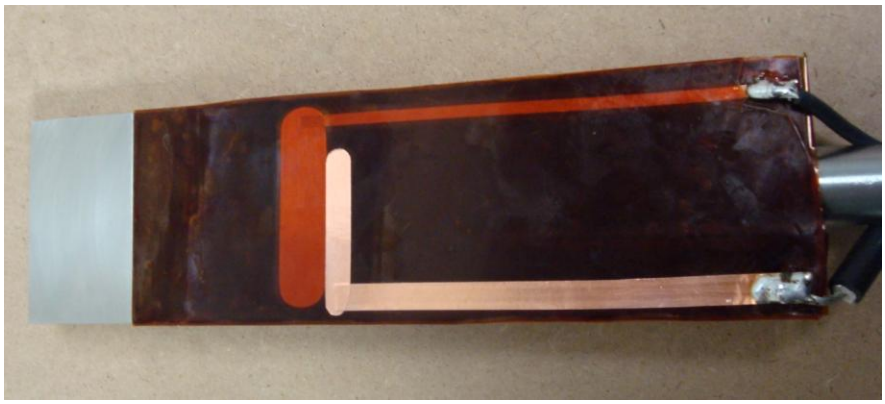

(a)

(c)

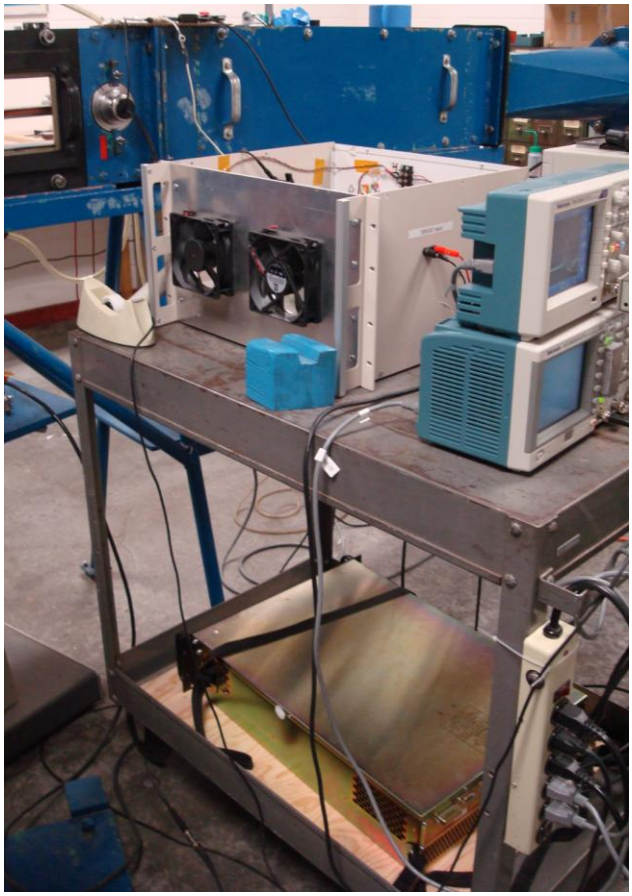

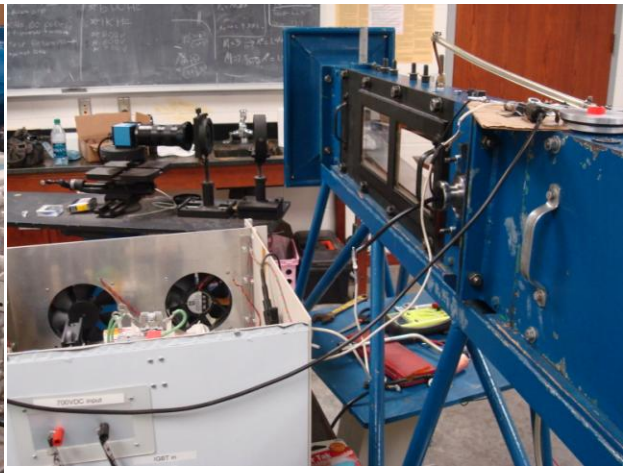

(b)

Fig. 4. (a) Flat plate with plasma actuator and electrical connections. (b) Electrical setup on cart. (c) Connection between actuators and cart setup

Because of the use of high voltages in generating plasmas, and as a result of the electrical components needed in the test section to actuate the plasma, a few unusual considerations had to be taken into account in the design of this plate. Though the plate was composed primarily of

steel, the back 6.75” of the top half of the upper surface was formed from a dielectric material that did not adversely interact with the plasmas generated or become highly electrically charged during use. The part of the plate with the dielectric layer was recessed compared to the front 1.25”, so its height was built up with additional dielectric Kapton tape. An actuator was constructed on and between these layers of tape, starting 3” back from the front tip of the plate. The electrodes were then extended (one on each side) to the back of the plate. Here, they were soldered to high voltage wires that passed through two small holes into the cylindrical tube. They proceeded through the tube and out through the thin cylinder in the side of the wind tunnel. From here, they connected to the typical actuator electrical setup. Images of this are shown in Figure 4.

This setup was required to generate the very short, high voltage pulses needed to create NS plasmas. Electricity from a high voltage wall outlet was pulled into a 700 V DC power source. This then connected to a specialized “pulser” that essentially chopped this DC energy into long pulses and then compressed them into ~100 ns long pulses. These pulses were released whenever an IGBT gate in the pulser was signaled by a square wave from a connected function generator. (More detailed specifications for the pulser can be found in Reference 7). The frequency of pulse release (which is the same as the frequency output by the function generator) is the frequency referred to in the latter parts of this study.

The NS pulses then passed into the wind tunnel, to the high voltage electrode on top of the flat plate. The electrical signal passed to the grounded electrode, which connected back to the pulser. An oscilloscope was connected in series and in parallel with the electrode to provide current and voltage data for each pulse (like that shown in Figure 1).

Besides these electrical data, the primary data collected in this study were pressure measurements at various points in the wind tunnel and schlieren images of the flow around the

flat plates. For the pressure measurements, one pressure tap each in the top and bottom of forward part of the test section were used to collect static pressure data (p), which was then used to calculate the Mach number of the flow with the ratio of p over the stagnation pressure p_o of the air pulled into the tunnel. Previous tests had been run comparing the Mach number from this calculation to that using the Pitot-static pressure measurement, as another aid in calibrating measurement of the flow speed. The imaging used in these experiments is called schlieren imaging. It uses the refractive properties of air to visually represent density gradients in the flow, which are predominantly caused by shocks and boundary layers, in this case.

III. Results and Discussion

Before tests were performed with the specially designed flat plate, another larger flat plate was used to characterize the supersonic wind tunnel when a comparable object was occupying the tunnel. This plate had the same basic geometry as the one used for plasma testing, but it had a larger area frontal cross-sectional area. As the specially-designed plate would be later, it was inserted into the test section parallel to the flow. Airflows with Mach numbers ranging from approximately 2 to 4 were then run through the tunnel. Schlieren images were taken with the flow in steady state to show shock angles and locations, and pressure measurements were taken to calculate flow speed. The results are shown in Figures 5 and 6.

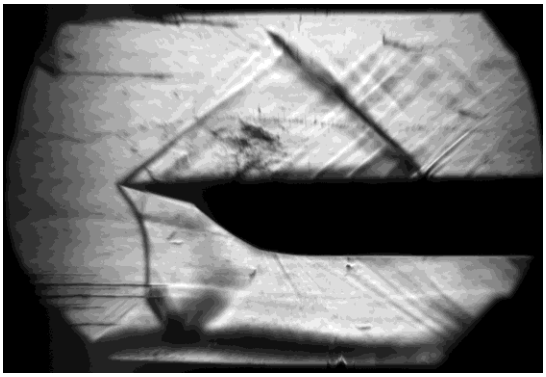

(a)

(b)

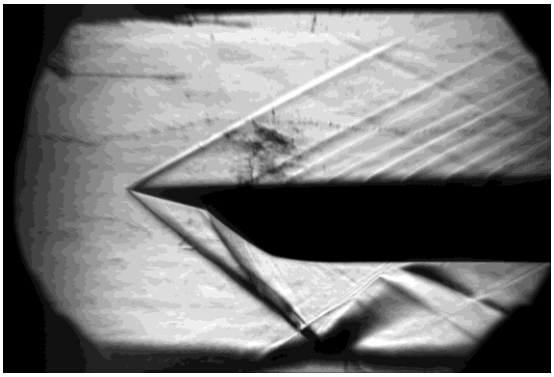

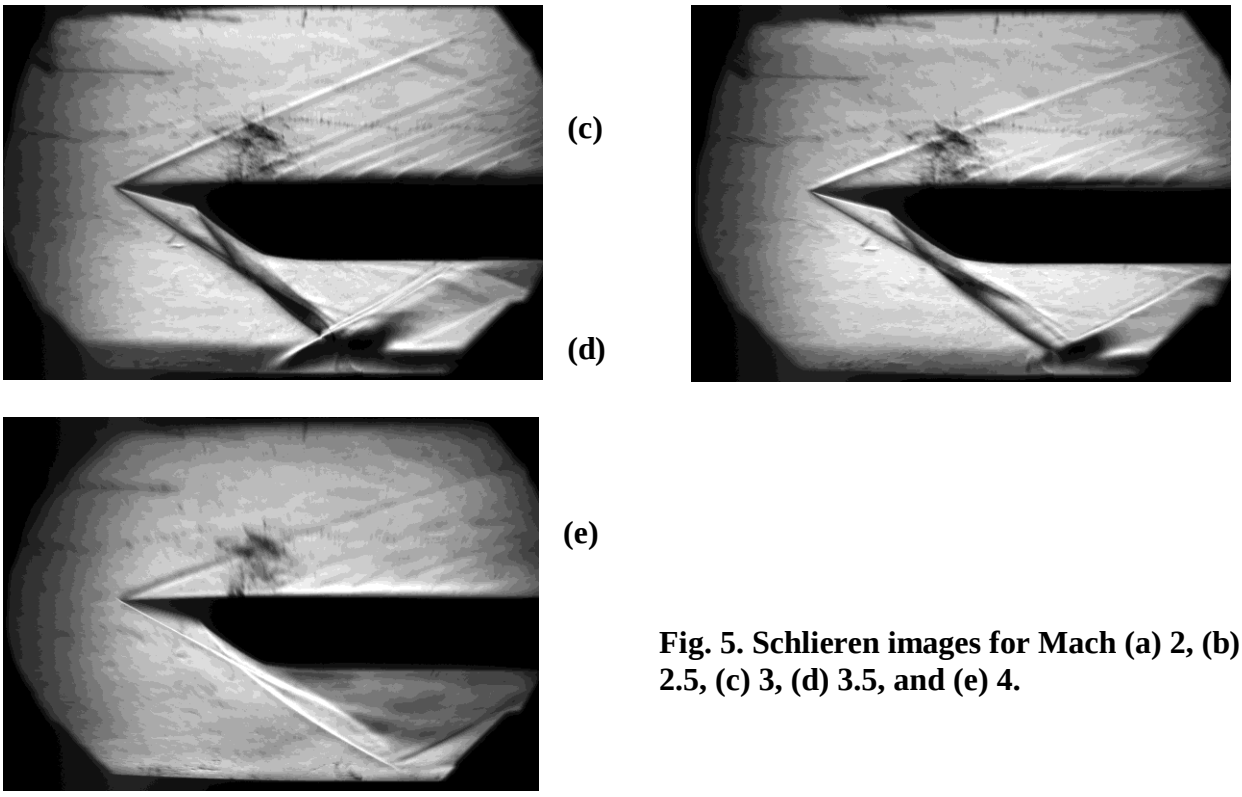

Fig. 5. Schlieren images for Mach (a) 2, (b) 2.5, (c) 3, (d) 3.5, and (e) 4.

The images in Figure 5 all show similar features. There are initial shocks at the front tip, one angling up over the top surface and the other extending below the plate. A secondary shock occurs on the underside where this plate meets its supporting cylindrical shape. Smaller shocks can be seen to occur where the flow encounters pressure taps—a number of these have been drilled into the top surface of this particular plate. Boundary layers can also be identified as the darker, less sharply-resolved area just above the top surface of the plate and the similar region above the floor of the wind tunnel in lower Mach number flows.

Though there are some similarities (and obvious differences like the angle the initial shocks make with the plate), there are also a few noticeable differences in the images for different Mach numbers. Figure 5(a) shows the most distinctive image, particular when the shocks beneath the plate are taken into account. There is a very large shock in this area that does

not yet mold to the form of the flat plate. There are also multiple shocks of varying strength at the front top of the plate, instead of a single strong shock, and the strongest shock shown has a definite reflection from the top of the wind tunnel. None of these features are particular desirable. The complications in the flow at this Mach number occur largely because of the blockage the flat plate causes in the test section. Its large cross-sectional area (when viewed from the perspective of the flow coming towards it) decreases the effective area of the test section. The Mach number of the flow is determined based on the ratio of the throat area of the converging nozzle and the cross-sectional area of the test section (referred to as the "area ratio"). Decreases the effective area of the test section decreases this area ratio, making it harder for the flow to reach supersonic speeds. As the actual area ratio increases, this blockage has less noticeable of an effect and the flow reaches the desired Mach number. This large frontal cross-sectional area was also one of the features the design of the new flat plate sought to improve.

The Mach number is listed in the label for Figure 5 is based on the area ratio setting of the wind tunnel during the test. However, due to flow imperfections and losses that occur in real flow and are not taken into account in flow speed calculations, this was not the actual Mach number that resulted. Approximations for the actual Mach number are made by calculating this number with several different methods and measurements. These are the results shown in Figure 6. The methods and measurements used (also listed on Figure 6) were: the p/p_o ratio, logarithmic best-fit lines from prior tests comparing Rayleigh-Pitot probe calculations to this p/p_o value, and the shock angle for the flow in each test. Because of the strong possibility for error in the pressure measurements taken, the shock angle Mach number is likely the most accurate. The fact that the angle Mach data points trend in a manner parallel to the area ratio Mach points

corroborates this. At high Mach, it is believed that leaks in the test section static pressure lines are causing errors.

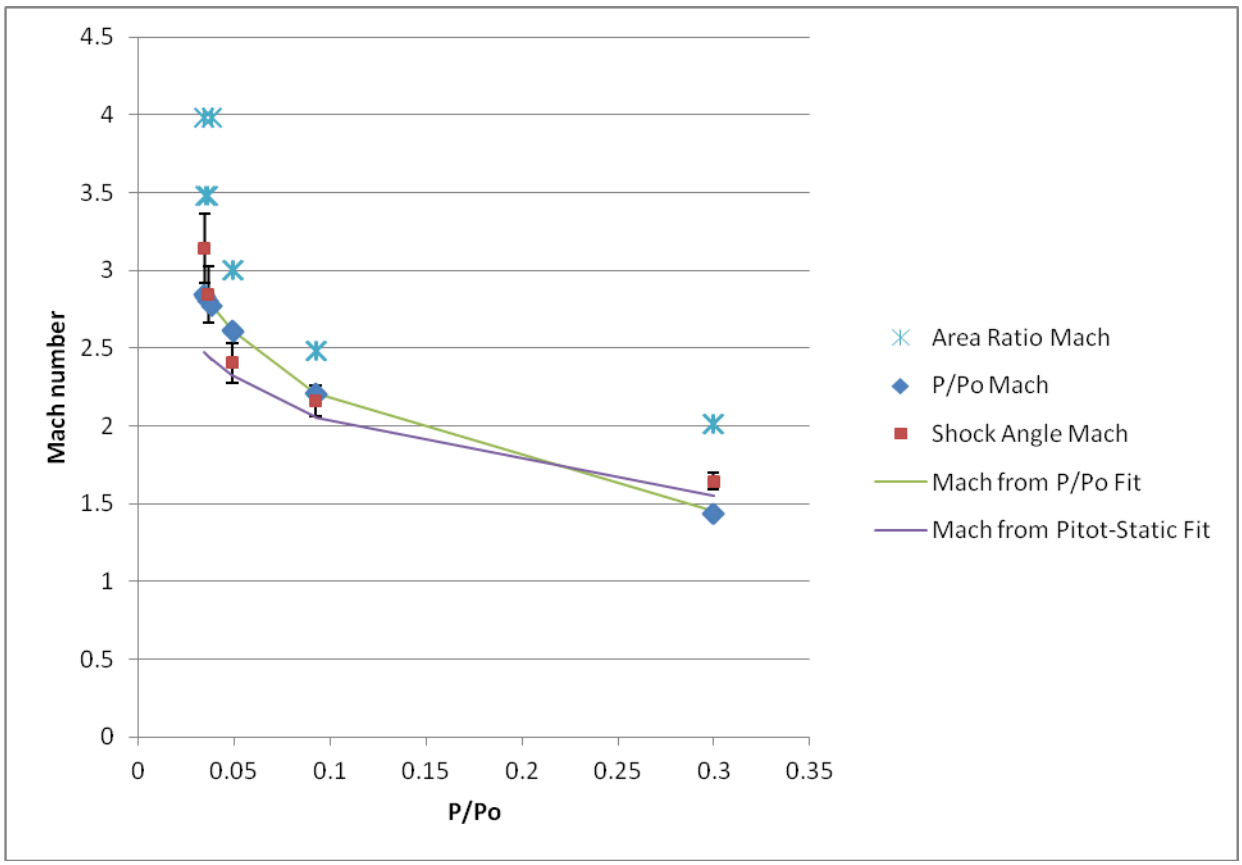

Fig. 6. Mach number for the flow was calculated multiple ways for each trial. Here, the numbers are shown on the y-axis with the p/p_o ratio for the trial on the x-axis. The legend gives the method used to calculate that particular value.

After these tests were performed, and once the new flat plate was obtained, tests with the plasma actuators could begin. However, many complications were encountered along the way. First of all, it was discovered that the holes in the plate apparatus that were open to outside air to allow electrical connections caused flow problems. High speed flow in the tunnel results in very low pressures, but these holes allowed a way for the wind tunnel to pull in outside air, causing some areas of supersonic flow and some areas of high turbulence. The resulting flow can be seen in Figure 7. This was fixed by adding the seal shown in Figure 3(c), attached with vacuum

grease. The flow was still inconsistent in reaching the desired Mach number in the entire test section, so eventually the area ratio was increased to provide higher Mach. The flow then started normally.

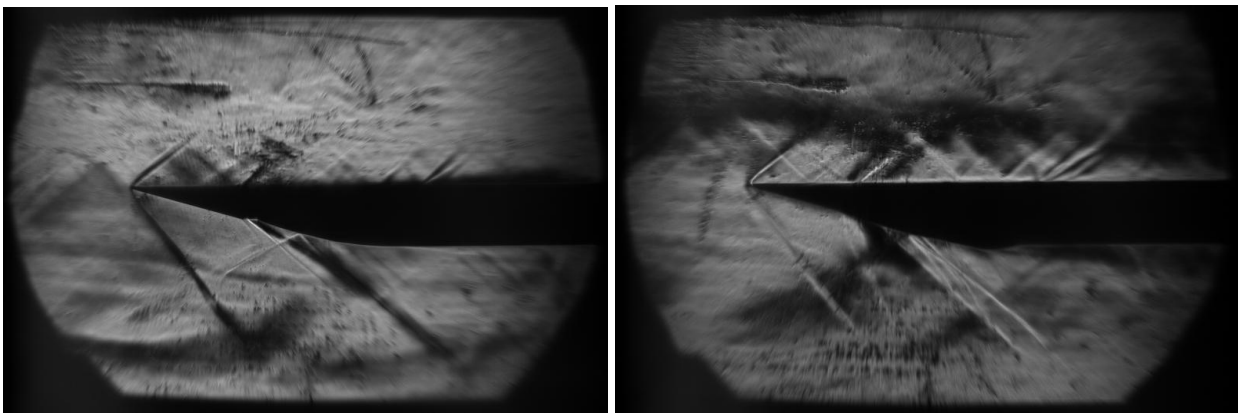

Fig. 7. Flow without an outside seal at the electrical connection exit. Same flow speed, but image on the right side has higher schlieren sensitivity to detect density gradients.

In the course of testing, it was also found that Kapton and copper tape actuators might not be the best design for use in supersonic flow. While the tape adhered well to the recessed dielectric surface of the plate, any tape that needed to wrap around the edge of the plate or fit over irregular geometries like the soldered electrical connections to the wires was at great risk of being dislodged by the air flow. When this occurred and the tape could move during the wind tunnel tests, it caused irregular flow similar to that which resulted from the lack of a seal in the wire exit area. An example is shown in Figure 8. This issue was remedied by using several thinner layers of tape to replace fewer thicker layers so that the tape could more closely follow the geometry of the plate and be less exposed to the forces of the flow.

Once these basic flow problems had been resolved, testing in the wind tunnel with plasma could begin. First, actuators were tested in the tunnel with the flow off, to ensure that the electrical connections were correct and the actuators were functioning normally. Images of this

stage can be seen in Figure 9. The light from the plasma can be seen, along with air disturbances caused by the heating and pressure waves that accompany it, as described in reference 3.

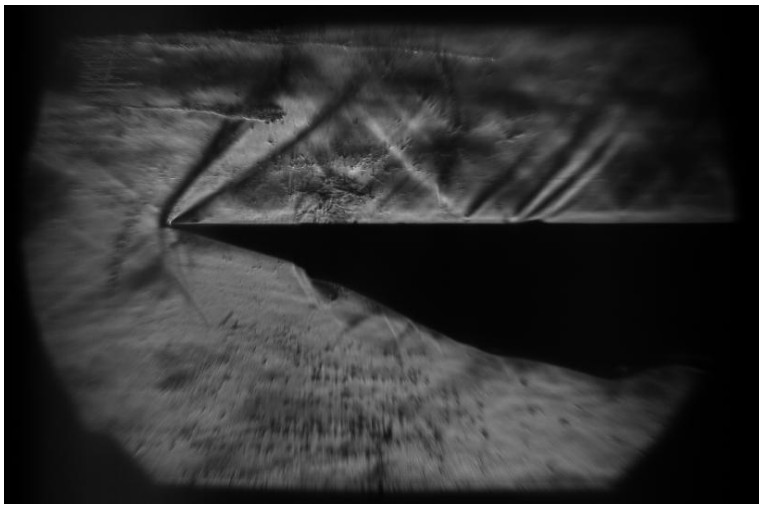

Fig. 8. Flow with dislodged tape movement. The plate appears larger than normal on the underside because of the tape blocking the schlieren image.

Then, the flow was started and the plasma was turned on after it stabilized. Initially, no images were taken, but the plasma was closely observed to see if it reacted unusually. The plasma was seen to arc from the free end of the high voltage electrode and was believed to be reaching over the edge of the tape to the metal plate (at this point, the tape configuration was like that shown in Figure 3(a)). This occurs due to the pressure decrease in the tunnel when running. In an attempt to address this, the bottom layers of tape were extended over edges and around to the bottom of the plate. This was tried first with 5 μm tape (which caused the issues described in and around Figure 8), and then with thinner tape closer to the sides so that the tape configuration was like that shown in Figures 3(b)-(c). The plasma was tested again in the flow, and an arc was observed from the high voltage electrode to the edge of the upper layers of Kapton tape. There was an air pocket through which it could reach the grounded electrode. The actuators were reconstructed with the grounded electrode further from the tape edge and with a layer of the tape between the electrodes extending over the edge of the plate to the bottom, and this fixed this particular arcing issue.

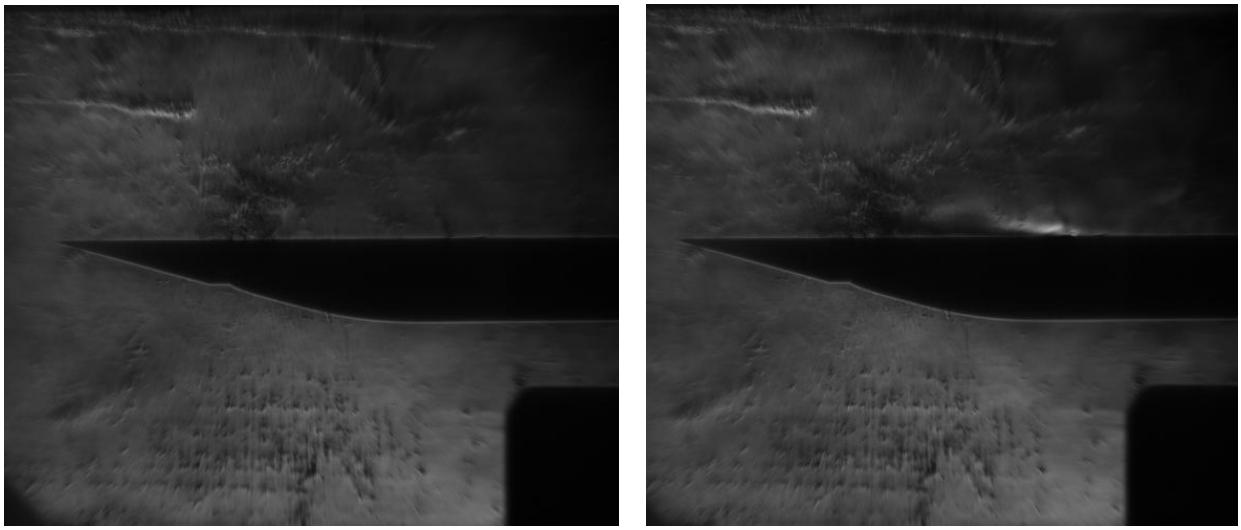

Fig. 9. Image on the right shows plate in still air with plasma running with an input voltage of 700 V and at a frequency of 1 kHz. For comparison, an image of plate in still air without plasma is on the left.

After this, plasma was tested in flow at Mach 2.4. For the first round of tests, the DC voltage was set to 500 V. The flow was started, and then ten images were taken with one second between each image. The first five images were of the flow in steady state, and then the plasma was started and ran as the last five images were taken. A sample sequence of these images is shown in Figure 10.

What was expected to be seen in these tests was a change in shock location or boundary layer thickness when the plasma was turned on. The different shocks, their known causes, and which one(s) we hoped would be affected are labeled in Figure 11. However, as shown in the first and last images when plasma would definitively be either on or off, no change was observed.

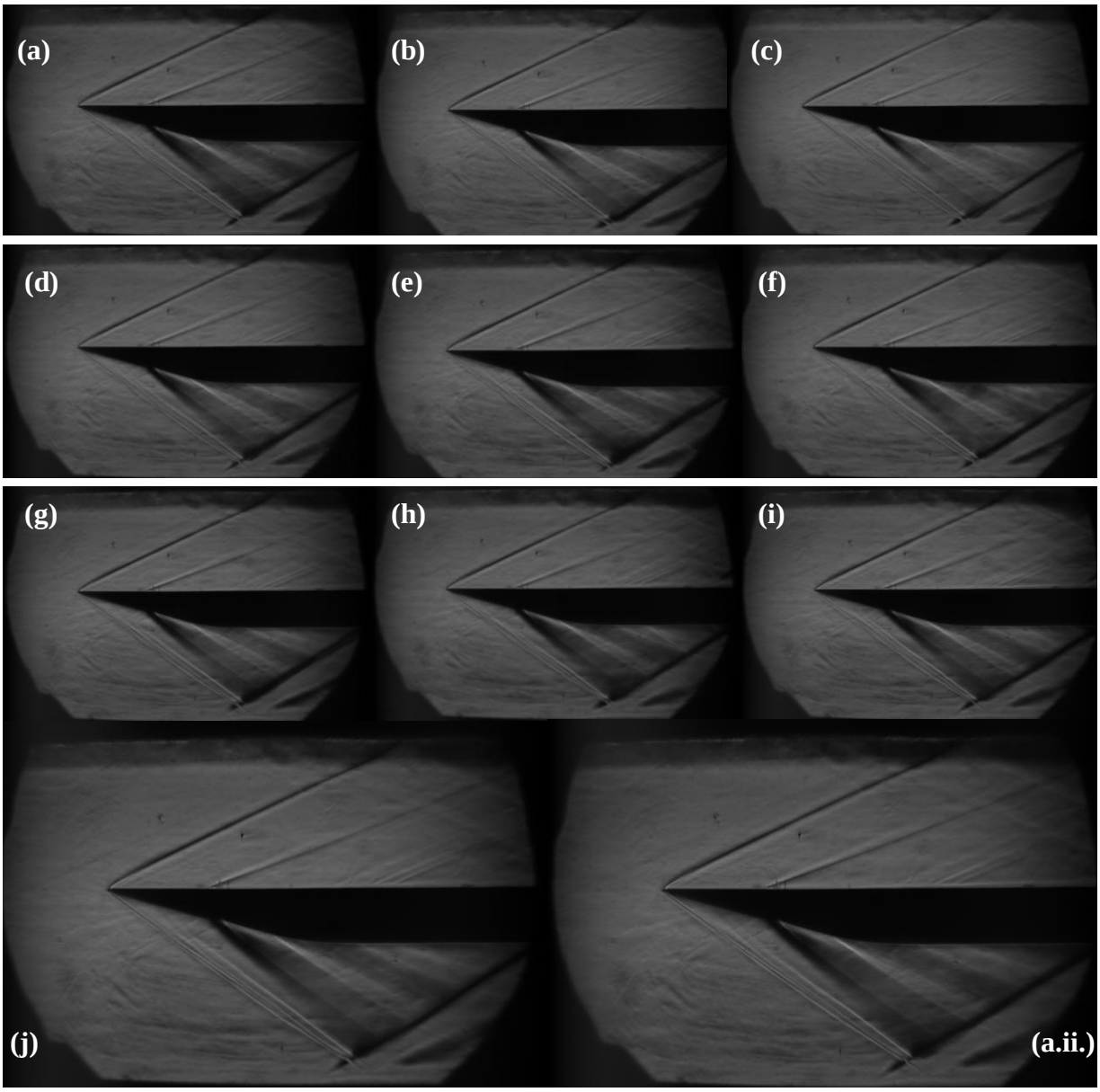

Fig. 10. Full sequence of images taken during one wind tunnel run. Images (a)-(e) show steady flow without plasma. Images (f)-(j) show steady flow with plasma set to 500 V and 500 Hz. For easier comparison, Image (j) is shown on the bottom left, and Image (a.ii.) on the bottom right is an enlarged version of (a).

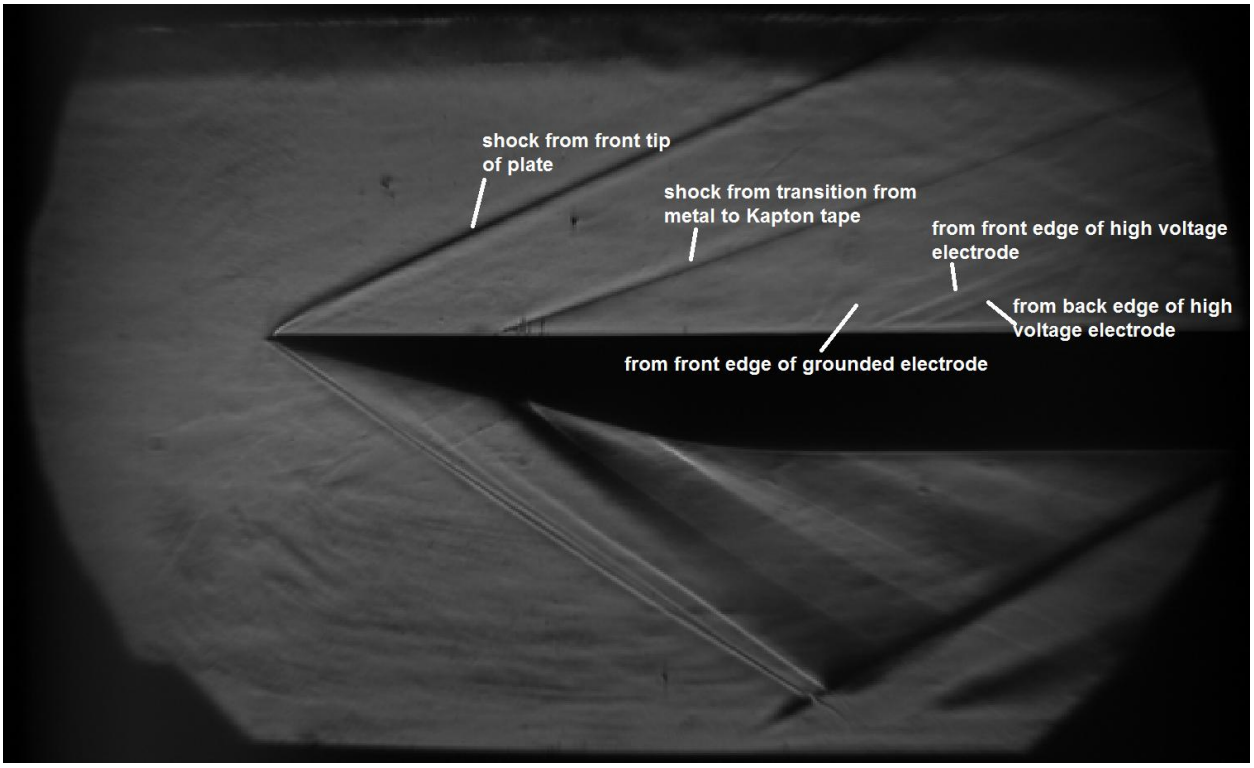

Fig. 11. Typical schlieren image at M=2.4. Flat plate shown with expected shocks. The relevant shocks from the top surface are labeled. The actuators were expected to affect the shock from the front edge of the high voltage electrode.

The next step was to repeat these tests with the plasmas generated by a higher input voltage. The tests were started again at 600 V, with frequencies of 10 Hz, 100Hz, and 500 Hz. Schlieren images were taken in the same fashion for the first two frequencies. Again, no change was noted in the shocks. However, the current as observed on the oscilloscope appeared to be higher than normal, but not as high was it normally reaches when there is a plasma arc on the actuator. The tests were repeated with no schlieren images taken, but with the plasma observed from a different angle. At 600 V and 500 Hz, plasma was seen to be arcing from the wire connections at the back to either the center cylinder, the metal bottom of the flat plate area, or between the ground and high voltage wires (because of the odd viewing angle, it was difficult to tell). This higher current is detrimental to the pulser and is also not delivering the intended energy to the flow, so once the problem was identified, tests at 600 V were stopped. A simple fix

was attempted by adding Kapton tape to insulate the nearby metal cylinder and plate areas, but the tape did not survive flow testing at these speeds because of the difficult geometries it had to navigate.

With this fix proving unhelpful, it was deemed necessary to see if this same problem had been occurring but gone unnoticed during the 500 V tests. The plasma in the tunnel was tested again at 500 V and 500 Hz, and the digital photograph shown in Figure 12 depicts the findings. As expected, the plasma is hottest and brightest at the edge between the two electrodes. Unfortunately, there are strong glows along the copper tape connections to the electrodes and around the connecting wires at the back. This could suggest that some of the energy intended to be channeled to the edge between the high voltage electrodes is being used to ionize air in the electrical path along the way and is therefore being lost. This could contribute to the lack of effectiveness seen at 500 V, and the loss effects would only increase as more of the electrical energy is lost due to arcing at higher voltages.

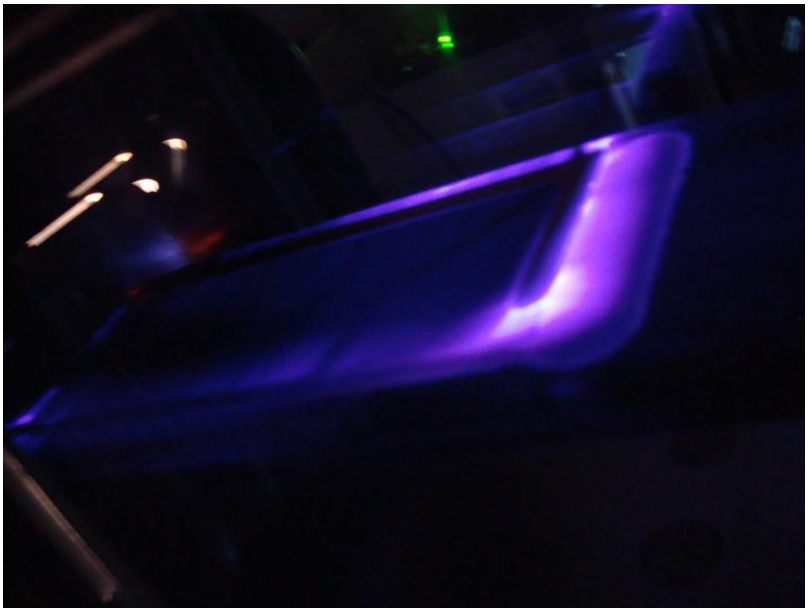

Fig. 12. Image taken in the wind tunnel with flow at M = 2.4. Plasma is shown as the purple glow in the image. Lights are off in the room to make the plasma easier to see.

IV. Conclusions and Future Work

Based on the schlieren images taken, plasma actuation with the configuration and electrical settings tested does not seem to be effective in altering shocks or boundary layers in supersonic flow. However, because of the narrow breadth of the tests run and the experimental/design challenges, this does not preclude effectiveness of the plasma under different conditions. With a few modifications, these actuators may yet prove useful in supersonic flow. Specifically, concentrating the plasma at the electrodes and eliminating the loss of energy elsewhere in the setup could drastically improve the effectiveness of the actuators. Besides that, they might function more effectively if the flow was set to a lower Mach number, or if the actuation occurred at a higher frequency or with a higher input voltage.

The tests performed and presented here did result in the discovery of a number of improvements that should be made for any future testing. The most important is the resolution of this arcing issue at the back, so that higher voltage tests can be run. This might be done by having the exposed wire connections shorter or insulating them with a high voltage epoxy. The extent of the plasma generation at areas other than the electrode should also be addressed. It was not expected, but it makes sense given that lower voltages are required to ionize air (and thus generate plasma) at lower pressures (which are almost always found in supersonic flows). Given this effect, more dielectric tape (or insulating epoxy) could be used to insulate the copper tape electrical connections and decrease energy loss from these areas. A much more drastic measure that might also be implemented in the future would be to construct the entire flat plate apparatus out of some non-conductive material, but this does not seem feasible at the present time given the difficulty of fabrication this would involve. All in all, much has been learned in this study

about the process of testing actuators in more extreme environments, and this will enable further, more productive tests to be undertaken in the future.

References

[1]Rethmel, C., Little, J., Takashima, K., Sinha, A., Adamovich, I. and Samimy, M., "Flow Separation Control over an Airfoil with Nanosecond Pulse Driven DBD Plasma Actuators," AIAA Paper 2011-0487, 2011.

[2]Moreau, E., "Airflow Control by Non-Thermal Plasma Actuators," Journal of Physics D: Applied Physics, Vol. 40, 2007, pp. 605-636.

[3]Little, J., Takashima, K., Nishihara, M., Adamovich, I., and Samimy, M. "High Lift Airfoil Leading Edge Separation Control with Nanosecond Pulse Driven DBD Plasma Actuators." AIAA Paper 2010-4256, 2010.

[4]Roupassov D., Nikipelov, A., Nudnova, M., and Starikovskii, A. "Flow Separation Control by Plasma Actuators with Nanosecond Pulsed-Periodic Discharge." AIAA Journal, Vol. 47, 2009, pp. 168-185.

[5]Greenblatt, D. and Wygnanski, I., "The Control of Flow Separation by Periodic Excitation," Progress in Aerospace Sciences, Vol. 36, 2000, pp. 487-545.

[6]Nishihara, M., Takashima, K., Rich, W. and Igor, A., "Mach 5 bow shock control by a nanosecond pulse surface dielectric barrier discharge," Physics of Fluids, Vol. 23, 2011, pp. 11.

[7]"High Voltage Pulse Generator User Manual." The Ohio State University Nonequilibrium Thermodynamics Laboratory. Ver.1, 2009.